INTERNATIONAL JOURNAL OF
COASTAL, OFFSHORE & ENVIRONMENTAL ENGINEERING

IJCOE Vol.11/No. 1/Winter 2026 (46-56)

Available online at: www. Ijcoe.org

Effects of bridge curvature radius on results of nonlinear dynamic analysis in coastal curved bridges

Shahrouz Arabestani[1], Mohammad Reza Mansoori[2*], Fereshteh Emami[3], Panam Zarfam[4]

Department of Civil Engineering, SR.C., Islamic Azad University, Tehran, Iran.

1- *0057059551@iau.ir*
2- *m.mansoori@iau.ac.ir (Corresponding Author).*
3- *femami@iau.ac.ir*
4- *zarfam@iau.ac.ir*

ARTICLE INFO

Article History:
Received: 07 Sep 2025
Accepted : 4 Jan 2026

Keywords:
seismic vulnerability, curved bridges, Curvature radius, BEP analysis, IDA

ABSTRACT

One of the methods that has appropriate accuracy, applicability and reliability and will be discussed in this study is the Bidirectional Energy Based Pushover (BEP) method. Because the capacity curve obtained from BEP is unique and the main parameters of the pusher (load pattern, control point and monitor point) cannot question the accuracy of this approach; because there is no need to select a point monitor to obtain the capacity curve and instead, all the monitor points must be displaced to calculate the energy absorbed in the pusher stage. This method has been evaluated in terms of accuracy and applicability in building structures. This is while the aim of this study is to extend this method to assess the seismic vulnerability of bridges with curvature in plan.

After identifying and selecting the methods and models considered for each element, and considering the defined uncertainties, the proposed models are modeled in OpenSeesPy software to perform IDA analysis. In order of material behavior, concrete, steel, geometry and modeling details, boundary conditions are selected based on previous studies, and modeling is performed accordingly. In this paper evaluated the effects of radius of curvature on the seismic response of curved bridges. For 4-span bridges, the weak and strong earthquake errors increase with increasing radius of curvature. However, for 2-span and 3-span bridges, the curved bridge with a radius of 420 m in two spans and the curved bridge with a radius of 1000 m in three spans experienced lower average errors in very strong motions (84th percentile) than the other curves. This indicates that the effect of curvature on accuracy depends on the bridge configuration. The errors between the BEP curve and the accurate IDA vary depending on the earthquake magnitude (percentiles). Weaker and stronger earthquakes (84th and 16th percentiles) generally showed higher errors compared to moderate intensity (50th percentile).

1. Introduction

A systematic investigation into the impact of the design parameters of bridges (e.g. the radius of curvature and the longitudinal slope) on their seismic pounding response is necessary. However, there have only a few studies on these kinds of parameters of curved bridges. Naseri et al. (2020) [1] investigated effects of curvature radius on vulnerability of curved bridges subjected to near and far-field strong ground motions. Analytical seismic fragility curves have been derived thru considering uncertainties in the earthquake records, material and geometric properties of bridges. The findings indicate that near-field effects reasonably increase the seismic vulnerability in this bridge sub-class. The results pave the way for future regional risk assessments regarding the importance of either including or excluding near-field effects on the seismic performance of horizontally curved bridges.

Jiao et al. (2021) [2] evaluated experimental and numerical investigations on the effects of radius of curvature and longitudinal slope on the responses of curved bridges subject to seismic pounding.
Because of the irregular geometries, earthquake-induced adjacent curved bridge pounding may lead to more complex local damage or even collapse. A series of parametric studies were then conducted to examine the impacts of the radius of curvature and longitudinal slope of the superstructure of the curved bridge on its seismic pounding response. The results show that the maximum pounding force first increases and then decreases as the radius of curvature increases, but that it decreases monotonically with the growth of the longitudinal slope. These results suggest that controlling the radius of curvature and the longitudinal slope of the superstructure of the bridge can reduce the localized high stress that is induced by seismic pounding. Also, the unevenly distributed pounding forces can significantly increase the relative radial displacement of the bridge's deck corners, although the relative tangential displacement may decrease. It is thus necessary to adopt effective anti-pounding measures to prevent the superstructure of the bridge from being unseated.
Wilson et al. (2014) [3] performed a comprehensive performance analysis on eight bridge configurations of various degrees of skew and curvature. Nonlinear time-history analysis is carried out on each bridge configuration using detailed finite element models. The results show the curved bridge models induced higher moment demand in the weak axis of the substructure and overall lower shear demand in comparison to the other configurations. Curvature also introduced higher moment demand on the interior pier-columns, which increased with lower radii. However, when the pounding effect is considered, these laws may not be applicable. Results stated the relationship between the radius of curvature and the displacement and force demands on the curved bridge. Result showed that the curvature radius of the bridge has a relatively small influence on the tangential displacement at the four corners. The induced difference was within 33%. In general, as the radius of curvature decreases, the tangential displacement at the corners slightly decreases, indicating that the pounding between adjacent girders has a constraining effect on the tangential movement of the bridges' deck. Such an effect always increases as the radius of curvature decreases. Compared with the tangential displacement, the curvature radius has more impacts on the radial displacement. Results showed that the radial displacement changed abruptly when the radius of curvature was larger than 100 m. When the radius of curvature is 100 m, the maximum radial displacement at the corners has reached approximately 4.5 times that of the straight bridge. As the results, the torsional response of the main girder changed significantly with the radius of curvature. Compared with the straight one, the horizontal and vertical rotation of the model with the radius of curvature of 30 m are up 22.4 times and 18.3 times, respectively. Overall, as the radius of curvature decreases, the horizontal and vertical torsional responses significantly increases, which could be detrimental to the structure.
Mirza Goltabar Roshan et al. (2021) investigated effect of curvature radius on probabilistic evaluation of seismic horizontally Curves RC Box girder bridges using Monte Carlo simulation under three-dimensional excitations under Near-Field Earthquakes [4].
Agrawal and Kumar Gupta (2024) evaluated effect of radius of curvature on the seismic response of curved bridges [5].

Figure 1: A coastal curved bridge (Laguna Garzon bridge in Uruguay).

2. Methods

IDA is one of the most reliable methods, especially in the case of irregular structures, to estimate the seismic response of structures. In addition to the complexity associated with the formulation of the mathematical model, other major issues arise with respect to the definition of the seismic load, which can lead to different levels of uncertainty in terms of the global and local responses of the structure. Therefore, pushover analysis (nonlinear static analysis), with less time and simple initial principles and while ensuring results with appropriate accuracy, can be a suitable alternative method.

One of the methods that has appropriate accuracy, applicability and reliability and will be discussed in this study is the Bidirectional Energy Based Pushover (BEP) method. Because the capacity curve obtained from BEP is unique and the main parameters of the pusher (load pattern, control point and monitor point) cannot question the accuracy of this approach; because there is no need to select a point monitor to obtain the capacity curve and instead, all the monitor points must be displaced to calculate the energy absorbed in the pusher stage. This method has been evaluated in terms of accuracy and applicability in building structures. This is while the aim of this study is to extend this method to assess the seismic vulnerability of bridges with curvature in plan.

After identifying and selecting the methods and models considered for each element, and considering the defined uncertainties, the proposed models are modeled in OpenSeesPy software to perform IDA analysis. In order of material behavior, concrete, steel, geometry and modeling details, boundary conditions are selected based on previous studies, and modeling is performed accordingly.

However, since this approach relies on the assumption that the seismic response of any structure can be considered as the sum of the responses to individual modal forces (Soleimani et al. (2018)) [6], the effective and at the same time sufficient number of modes for the structure must be investigated. To do this, BEP is performed on the leading curve bridge for different numbers of modes.

In this section, we first introduced the class of bridges under study, and then discuss the details of modeling the substructure (columns and foundation), abutments, and deck.

The class of bridges studied in this study, based on the studies of Arajo et al. (2014) [7], Pinto et al. (1996) [8], Akbari (2012) [9] and Tehrani and Michel (2021) [10], has the following characteristics:

- Number of piers one, two and three respectively for two, three and four span bridges
- Height of piers 7, 14 and 21 meters
- Variable span length (100, 150 and 200 meters respectively for two, three and four spans and the length of each span is fixed and equal to 50 meters)
- Continuous deck (two, three and four spans)
- Deck width 14 meters
- Angles of curvature in the horizontal plane for two, three and four span bridges are equal to 130, 240, 420, 700 and 1000 meters respectively

Direction Modeling The reference bridge model tested in the Elsa laboratory by Pinto et al. (1996) [8] was used (Figure 2). This model was a straight bridge and all its geometric characteristics were used for modeling this research.

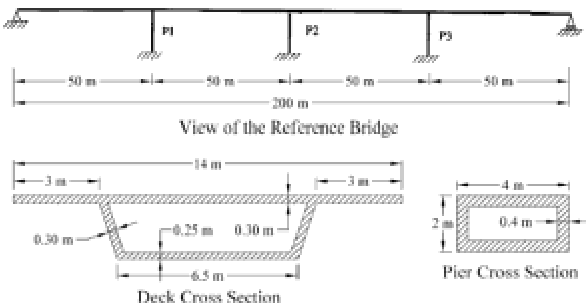

Figure 2: Configuration and details of the bridge studied by Pinto et al. (1996) at the Elsa Laboratory [8].

Reinforced concrete columns with a rectangular hollow section in the OpenSeesPy software must be modeled as Nonlinear Beam Column. Therefore, fiber has been used to consider the nonlinear behavior of the columns. On the other hand, the element used to model the columns is displacement-based beam-column elements. The cross-section of the columns in OpenSeesPy is defined as fiber elements to allow for the formation of a plastic hinge widely across the cross-section of the member.

Element: Displacement-based beam-column elements are used to model the columns, which allow the formation of plastic hinges in each part of the element. The upper and lower parts of the column, in other words, the connection between the top of the column and the deck and the base of the column and the foundation, are modeled using rigid elements to enable the transfer of moment and force between these members. To create the rigid element in OpenSeesPy, elastic beam-column elements with very high stiffness are used (because we expect the deck to remain elastic during an earthquake).

In the modeling, the columns are divided into 10 parts (mesh). It is worth noting that due to the symmetry of the columns, the consideration of rotational mass has been omitted (because the columns do not have eccentricity). Figure 3 shows the discrete finite element model of the single columns that has been studied.

Mass: Since the columns are fiberized and divided into 10 parts, half the mass is allocated to the first and last nodes (nodes 1 and 10) and the full mass is allocated to the remaining nodes (nodes 2 to 8).

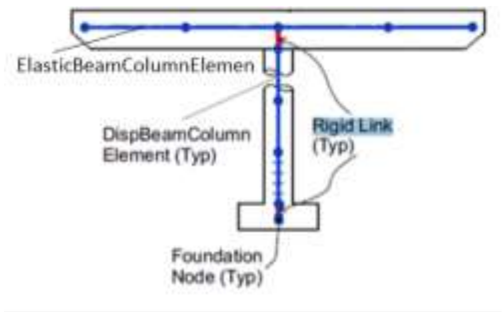

Figure 3: Single column discrete finite element model (schematic).

Bridge foundation modeling in OpenSeesPy: According to studies and information collected from the bridge maps studied by Ramanathan [11], a significant percentage of bridges, both in the middle frames and in the abutments, have extensive foundations supported by cast-in-place reinforced concrete piles. The structural system of the foundation consists of several vertical piles with a cap (the cap is modeled with a rigid element).

Materials: In this study, Uniaxialmaterials were used for the rotational and translational springs. For the rotational springs of two-span bridges, a value of 6.5×107 kip.in in radians has been assigned, and for three- and four-span bridges, no value has been assigned due to the articulated construction of the column footings (this information is based on the data and research of Ramanathan et al. in 2012 [12]). For the translational spring of two-span bridges, a value of 1400 kip/in has been used, and for three- and four-span bridges, a value of 1200 kip/in has been used (Ramanathan (2012)) [12].

Element: In OpenSeesPy, two coincident nodes are connected using the zeroLength element. In the present study, this element has been used to build the foundation model.

Mass: In this study, the calculation of the mass of the foundation has been omitted (based on technical literature).

Deck modeling: The height of the reinforced concrete box of the bridge decks under study is considered to be 2.3 m, based on the research of Pinto et al. [8] in 1996, which was carried out at the Elsa Laboratory. The width of the deck is also considered to be 14 m, and the geometric characteristics of the deck are modeled according to the reference model in the SAP2000 software. According to Figure 4, the box and single-cell decks are modeled. As can be seen in Figure 5, the box deck of the bridge class under study is modeled with one cell.

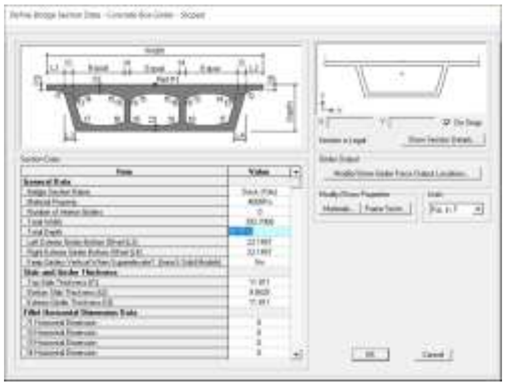

Figure 4: Deck specifications of the studied bridge class.

Based on these details, the cross-sectional area parameters and moment of inertia of the box-shaped deck of the bridges in two different directions (strong axis, Y and weak axis Z) were calculated and assigned to the elastic beam-column element of the deck in the OpenSeesPy software. Figure 7 shows the analytical deck model of one of the bridge models under study (a two-span bridge with a radius of 130 m) in the OpenSeesPy software, displaying the nodes in the longitudinal direction (20 nodes) and in the transverse direction (7 nodes for each section).

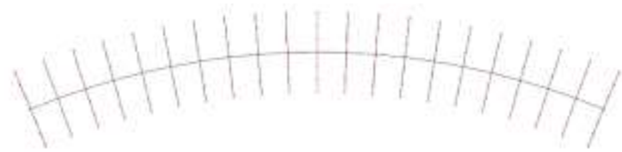

Figure 5: Analytical model of a box deck of a two-span bridge with a radius of 130 meters in OpenSeesPy software

The mechanical specifications of the deck are the same as the reference model and are considered as follows for deck modeling (unit kN, m):

fc=42.0e6

Ec= 2.5e10

Gc= 1.0e10

IzDeck=88.4

IyDeck=5.36

JDeck=11.7

ADeck=6.96

A three-line model based on the model proposed by Choi (2002) was used to model the behavior of piles [13]. It is worth noting that in this study, the bridge class with integral keel was used for modeling and according to the reference model, there is no gap between the deck and the keel and the effect of the side walls was ignored in this study. In the modeling, the keel was divided into seven equal parts on each side and a tangential and a radial spring were assigned perpendicular to each node. The ZeroLength element was used for the springs.

Figure 6 shows a representation of the 70PC class pile model. It is worth noting that only the pile stiffness, K, which is a constant value and is obtained from the derivative of the slope of the line in Figure 8, is considered in the modeling (the pile stiffness is modeled with a spring).

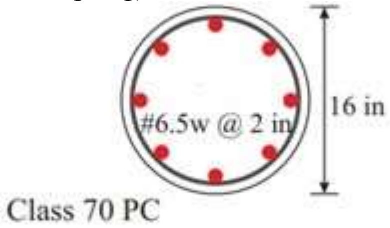

Figure 6: 70PC class pile model where only the pile stiffness, K, is used in the modeling with a constant value (Ramanathan 2012) [12]

It is worth noting that in the X direction (degree of freedom 1) the piles and the backfill soil are considered parallel, and in the Y direction (degree of freedom 2) we have only the piles.

Figure 7 shows the finite element model of a four-span curved bridge. In this figure, the deck, along with the longitudinal and transverse elements, abutments, columns, and bridge foundation, are defined with materials, and the details are shown along with the behavior of the relevant materials.

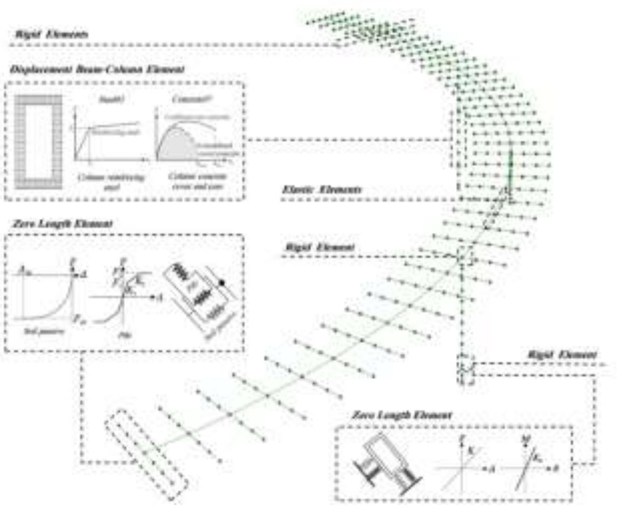

Figure 7: Finite element model of a four-span curved bridge

Study Bridges

Three-dimensional analytical modeling of the study bridges was performed in the OpenSeesPy software based on the analytical models presented by Pinto et al. (1996) [8], Araujo et al. (2014) [7] and Ramanathan (2012) [12]. It was performed by considering 5 radii of curvature (130, 240, 420, 700, and 1000 m) in the horizon line for the plan of the study bridges [11], different numbers of spans (two, three, and four spans), earthquake impact angles (0, 45, and 90 degrees), and 22 different FEMA-P690 earthquake records from g0.1 to g3.7. Two main reasons can be given for choosing these different curvatures, the first reason is the significant difference in their dynamic response (due to the change in the structural structure of these models) and the second reason is the difference in the correspondence between nonlinear static analysis (push-pull analysis) and nonlinear dynamic analysis (nonlinear time history analysis). The reason for choosing different numbers of spans is that by changing the model, the angle of curvature, θ, (θ = L/R, L is the length of the deck and R is the radius of curvature) changes, which causes a change in the dynamic response of the structure. On the other hand, the reason for choosing different angles of impact of earthquakes is the angle of the bridge structural members such as the girders, columns and deck, relative to the general axis. For example, by changing the local axes or the strong axis of the columns or girders relative to the general axis, a change in the dynamic response of the structure may be obtained, which should be investigated. The nomenclature and geometric specifications of the 15 bridge classes studied are described in Table 1 for radii of 130, 240, 420, 700 and 1000 m in the two-, three- and four-span bridge classes, respectively.

First step: First, all the mechanical parameters of the members (including the cross-sectional area of the reinforcement, compressive strength, elastic modulus of concrete and steel materials, yield strength of steel, etc.) and uncertainties of the applied seismic force (including earthquake characteristics and properties) are identified and modeled to build a model for fragility assessment. In addition, the capacity functions and limit state functions of the types of bridge elements that are necessary for fragility assessment are also studied and extracted from technical references. In this step, methods for selecting appropriate earthquake records are also discussed, and accordingly, appropriate earthquakes are selected from the existing earthquake collection based on scientific and appropriate methods to perform probabilistic seismic vulnerability assessment of bridge models. For this purpose, a set of 22 pairs of far-field earthquake records (FEMA P-695) is used.

As shown in Figure 1, the record set covers a diverse spectrum of earthquakes with significant effects, including variations in duration and frequency content (16th, 50th, and 84th percentiles). This diversity helps to create a more general dataset for the training algorithm in the following chapters.

Step 2: Based on the objectives of this research, in this step, curved bridges in plan are carefully and thoroughly studied in the technical literature and the effects of irregularities on the seismic behavior of various bridge members are identified. In this section, an attempt is made to identify the factors that have a greater impact on the results of fragility analysis so that these factors can be used in the subsequent sections where rapid methods are to be developed. In addition, definitions and values of bridge curvature available in the technical literature are identified and, based on this, curvature angles are selected and used to model curved bridges in the plan.

Step Three: Performing fragility analysis on all probabilistic models constructed in the first step and based on the selected irregularity levels, regular and irregular models are produced in the second step. All these regular and irregular models produced are subjected to IDA by the set of earthquakes selected in the first step and then its results, along with the capacity functions determined in the first step, are used for fragility analysis. In this step, first, the factors affecting the behavior of irregular bridges will be investigated and their fragility values will be compared with the aim of identifying the factors affecting the seismic behavior of irregular bridges. On the other hand, the results of this step will be used to validate the rapid method discussed in this study. Step Four: In this step, fragility analysis is performed for probabilistic models built based on selected irregularity levels using the probabilistic capacity spectrum method and considering record-to-record changes. In this step, using the IDA results in the third step, the validity and accuracy of this method are evaluated and then, in accordance with the factors identified in the first and second steps, this method will be improved and modified based on the reliability capabilities of this method for the model of bridges with curvature in plan.

One of these simple and practical methods is the Bidirectional Energy Pushover (BEP) method. This method uses the work done by lateral loads and moments, through Pushover analysis, as an index to determine the characteristics of modal single-degree-of-freedom systems. The proposed formulation of this method allows for the simultaneous effect of both components of ground motion in each mode. To combine the modal responses of this method, a modified perfect quadratic combination (CQC) method is also presented, which is specifically developed for two-component excitations. The accuracy of this proposed method is investigated on a two-way asymmetric three-story building. The findings show that BEP is able to estimate the two-component IDA results with sufficient accuracy. A bilinear energy-based pushover analysis has been developed to approximate the two-component IDA curves for buildings that are asymmetrical in plan. BEP applies both components of a ground motion simultaneously to each mode and uses a modified CQC combination rule to combine the modal responses. In addition, the energy-based approach used in BEP eliminates the possibility of changes in the pushover curve in the capacity curves. These features minimize the impact of the complexities associated with asymmetry in buildings and the two-component nature of the ground motion on the accuracy of BEP. In this study, the intention is to use this method to estimate the response of irregular bridges in plan and to evaluate its performance.

Step 5: In this step, the results of the rapid fragility analysis method are evaluated and compared, and its solutions, limitations, and advantages are stated. On the other hand, the parameters and factors affecting the results of the fragility analysis of curved bridges in plan are discussed and suggestions are made to improve the performance and also increase the accuracy of the rapid method.

In summary, the set of necessary measures to reach the fragility curves in this study is as follows:

• Collecting a set of earthquakes that indicate the risk of areas with high seismicity and include a wide range of severity criteria

• Building three-dimensional nonlinear analytical models using analytical models of various bridge members

• Determining critical members by performing a deterministic analysis on the model

• Building probabilistic models of seismic demand for each member at each angle of curvature of the bridge

• Using a combination of descriptive and prescriptive approaches in building limit state models

• Drawing system fragility curves for different angles of curvature of the bridge for different angles of impact.

In this study, considering the variety of structural analysis methods for estimating seismic demand, in addition to a complete description of how to model the nonlinear behavior of elements and configure the hollow section bridge system, nonlinear analysis methods such as nonlinear statics and IDA on bridge structures are investigated and evaluated. In addition, the IDA method under two-component ground motions has received less attention as a requirement for evaluating curved bridges in plan. Therefore, to fill this study gap, this study has presented a method for approximating two-component IDA in bidirectional energy-based Pushover analysis (BEP).

Table 1: 22 different FEMA-P695 earthquake records used in this study from 0.1 g to 3.7 g.

	Ground Motion X Dir		
	GMPath	dt	NPTS
1	YER360.AT2.txt	0.02	2200
2	TCU045-E.AT2.txt	0.005	18000
3	SHI000.AT2.txt	0.01	4096
4	RIO360.AT2.txt	0.02	1800
5	PEL180.AT2.txt	0.01	2800
6	NIS000.AT2.txt	0.01	4096
7	MUL009.AT2.txt	0.01	2999
8	LOS000.AT2.txt	0.01	1999
9	HEC000.AT2.txt	0.01	4531
10	H-E11140.AT2.txt	0.005	7807
11	H-DLT352.AT2.txt	0.01	9992
12	G03000.AT2.txt	0.005	7989
13	DZC180.AT2.txt	0.005	5437
14	CLW-LN.AT2.txt	0.0025	11186
15	CHY101-E.AT2.txt	0.005	18000
16	CAP000.AT2.txt	0.005	7991
17	BOL000.AT2.txt	0.01	5590
18	B-POE360.AT2.txt	0.01	2230
19	B-ICC000.AT2.txt	0.005	8000
20	ARC000.AT2.txt	0.005	6000
21	ABBAR--L.AT2.txt	0.02	2676
22	A-TMZ000.AT2.txt	0.005	7269

Table 2: Nomenclature and geometric specifications of the 15 bridge classes studied

Row	Class of bridge	Number of spans	Number of columns per frame	Angle of curvature in line with the horizon (degrees)	Span length (m)	Deck width (m)	Column height (m)
١	2 Span-130	٢	١	١٣٠	١٠٠	١٤	٧
٢	2 Span-240	٢	١	٢٤٠	١٠٠	١٤	٧
٣	2 Span-420	٢	١	٤٢٠	١٠٠	١٤	٧
٤	2 Span-700	٢	١	٧٠٠	١٠٠	١٤	٧
٥	2 Span-1000	٢	١	١٠٠٠	١٠٠	١٤	٧
٦	3 Span-130	٣	١	١٣٠	١٥٠	١٤	٧ ، ١٤
٧	3 Span-240	٣	١	٢٤٠	١٥٠	١٤	٧ ، ١٤
٨	3 Span-420	٣	١	٤٢٠	١٥٠	١٤	٧ ، ١٤
٩	3 Span-700	٣	١	٧٠٠	١٥٠	١٤	٧ ، ١٤
١٠	3 Span-1000	٣	١	١٠٠٠	١٥٠	١٤	٧ ، ١٤
١١	4 Span-130	٤	١	١٣٠	٢٠٠	١٤	٧، ١٤ ، ٢١
١٢	4 Span-240	٤	١	٢٤٠	٢٠٠	١٤	٧، ١٤ ، ٢١
١٣	4 Span-420	٤	١	٤٢٠	٢٠٠	١٤	٧، ١٤ ، ٢١
١٤	4 Span-700	٤	١	٧٠٠	٢٠٠	١٤	٧، ١٤ ، ٢١

۱۵	4 Span-1000	٤	١	١٠٠٠	٢٠٠	١٤	٢١ ، ١٤ ،٧

The column arrangement for the two-span bridge class is 7 meters, for the three-span bridge class, 7 and 14 meters respectively from left to right, and for the four-span bridge class, 14, 7 and 21 meters respectively from left to right (known as the P213 bridge in previous studies).

In the OpenSeesPy software, the fiber model has a unique feature that allows the definition of materials with different characteristics at different points of the cross-section. For example, the characteristics of unconfined concrete can be assigned to the concrete cover and confined concrete to the concrete core. In addition, the location of the reinforcements along with their diameters on the fiber cross-section are specified and the characteristics of the steel used in the longitudinal reinforcements are assigned to them. In the present study, the fiber model has been used to model the nonlinear behavior in columns.

In this study, the behavior of the concrete of the bridge components was modeled using the Concrete07 material, which is the newest material type available in the OpenSeesPy software. This material uses the Cheng and Mander (1994) model [14] to define the stress-strain curves for confined and unconfined concrete. This model is based on statistical analysis of laboratory Concrete07 material was used to model concrete in the OpenSeesPy software, which uses the Cheng and Mander model [14]. The method for obtaining its parameters for unconfined and confined concrete is given below [17].

Table 3: Specifications of the concrete used [17].

Parameters	values
(E) Modulus of elasticity (GPa)	30.5
Concrete Compressive (f'_c) Strength (MPa)	42
Tensile Strength (MPa) (F_t)	Waste
Strain at Maximum Compressive Stress	0.002
Confinement Factor	1.2
Specific weight (kN/m^3)	24

data obtained from cyclic compression tests conducted by a number of researchers.

Figure 8 shows the stress-strain curves of concrete in different unconfined and confined states with different stirrup spacings. The reinforcement of the bridge components was also modeled using the Steel02 material available in the OpenSeesPy software. This type of material uses the model of Mangoto and Pinto (1973) [15], modified by Filippo et al. (1983) [16], and is also capable of modeling isotropic strain hardening in steel.

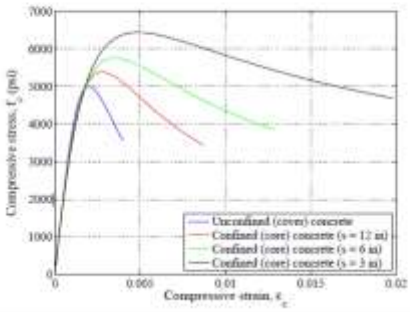

Figure 8: Comparison of concrete behavior curves at different levels of confinement

Table 4: Characteristics of steel used [17].

Parameters	values
(E) Modulus of elasticity (GPa)	200
(Fy) Yield stress of steel (MPa)	500
Strain hardening parameter (b)	0.005
Primary parameter of the shape of the transfer curve (a1, a2)	20
Transition curve calibration shape coefficients (a3, a4)	18.5 , 0.15
Isotropic hardening calibration coefficients	0 , 1
Specific weight (kN/m^3)	77

The constants Xn and Xp for confined concrete are taken to be 30 and 2 [18] according to figure 9.

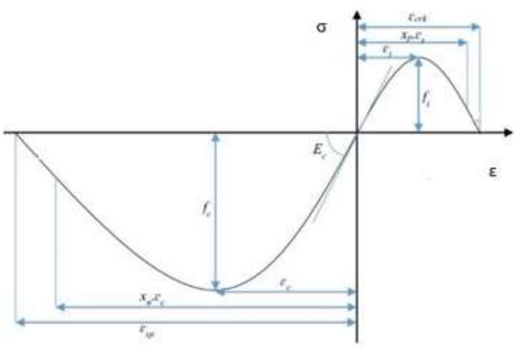

Figure 9: General stress-strain diagram used in Concrete07 materials (not to scale) [18].

3. Results and Discussions

In this study, the results discussed are used to complete the proposed framework, which leads to a fragility curve with low computational cost and high accuracy. For this purpose, the estimated EDP in the BEP and IDA results is converted into damage levels. In addition, 7 earthquake parameters are defined to determine stronger, milder or weaker earthquakes, as the results show that the accuracy of BEP varies between these classifications. Two structural features (radius and length) are used in the training process to predict the IDA damage levels along with 8 other features as figure 10.

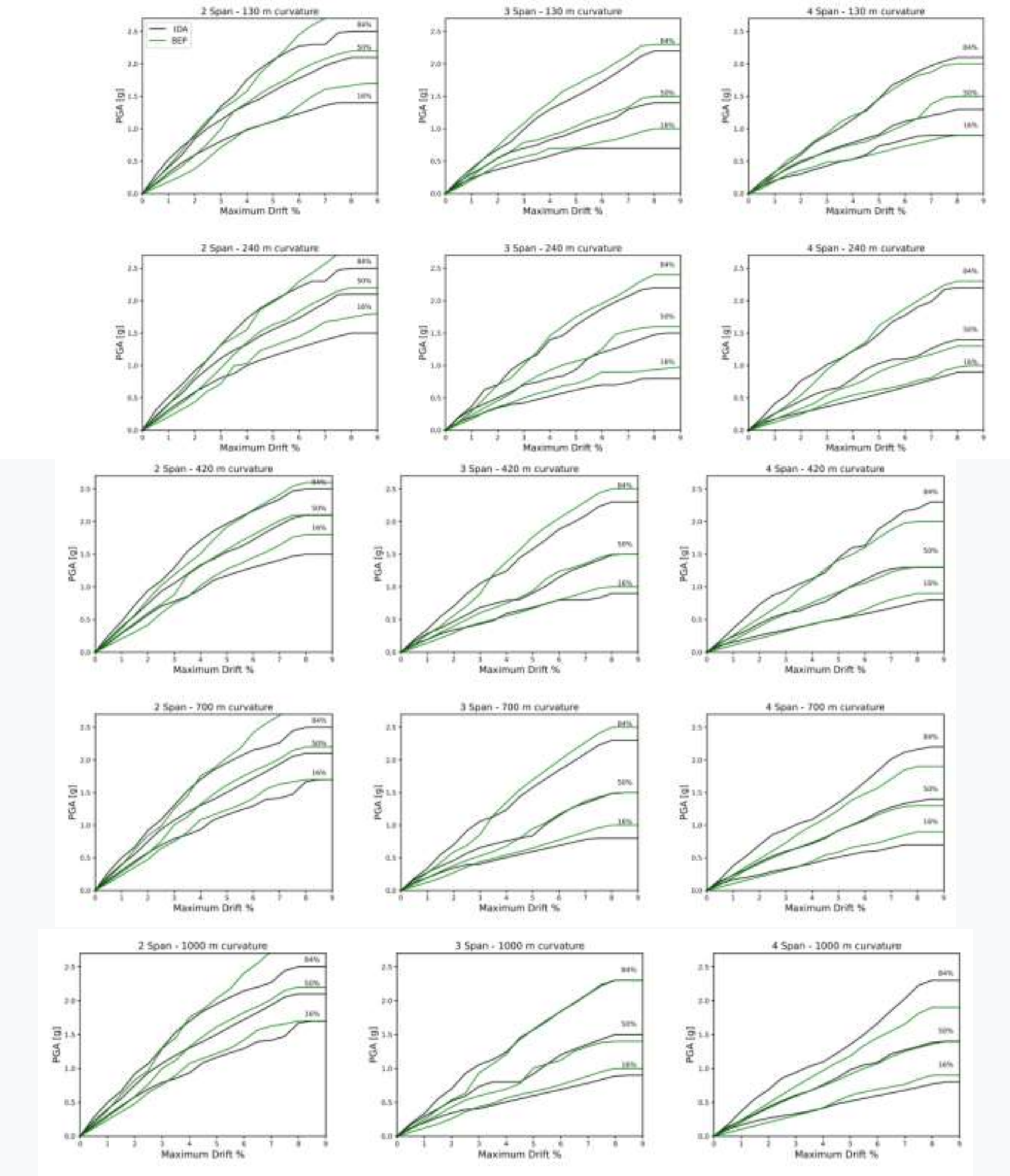

Figure 10: Results of BEP with two modes in a set of curved bridges

4. Conclusions

This research introduces a new framework for seismic performance assessment of complex structures. The framework achieves high accuracy and significantly reduces the computational burden associated with detailed finite element models. This study uses a set of distinct RC curved bridges to validate the accuracy of the framework through comparison with incremental dynamic analysis (IDA), which serve as examples of complex structures. To generalize the approach, the set includes curved bridges with important differences, including different curvatures, number of spans, and column height configurations. In addition, earthquakes with variations in amplitude, duration, and frequency content are selected to consider the effects of different earthquake strengths. First, the framework uses a bidirectional energy-based pushover (BEP) analysis to approximate the behavior of the structure. In this study, BEP is specifically extended for curved bridges to represent the nonlinear behavior of curved bridges with low computational costs. The accuracy of this method was observed by evaluating the following results:

• The relationship between bridge curvature and BEP accuracy appears to be complex, and other factors such as the number of spans and column height also play an important role. For 4-span bridges, the weak and strong earthquake errors increase with increasing radius of curvature. However, for 2-span and 3-span bridges, the bridge with moderate curvature (420 m) showed the lowest error. This indicates that the effect of curvature on accuracy depends on the bridge configuration.
• The errors between the BEP curve and the accurate IDA vary depending on the earthquake magnitude (percentiles). Weaker and stronger earthquakes (84th and 16th percentiles) generally showed higher errors compared to moderate intensity (50th percentile).

At radii of curvature of 130 and 240 meters, the values of the 84% damage level with the IDA and BEP methods are closer to each other, and with increasing the radius of curvature to 420 meters, 700 meters, and 1000 meters, the results of the maximum relative displacement at the 84% damage level differ more from each other, and the results in the four-span case at the 84% damage level with the BEP method are lower than with the IDA method.

Results by Wilson et al. (2014) [3] showed that the radial displacement changed abruptly when the radius of curvature was larger than 100 m. When the radius of curvature is 100 m, the maximum radial displacement at the corners has reached approximately 4.5 times that of the straight bridge. As the results, the torsional response of the main girder changed significantly with the radius of curvature. Compared with the straight one, the horizontal and vertical rotation of the model with the radius of curvature of 30 m are up 22.4 times and 18.3 times, respectively. Overall, as the radius of curvature decreases, the horizontal and vertical torsional responses significantly increase, which could be detrimental to the structure.

In this paper, by increasing the radius of curvature from 130 meters and above, we achieve the highest relative displacement for smaller values of PGA. By increasing the number of spans at a fixed radius of curvature, we achieve the highest relative displacement for smaller values of PGA. These results confirm the results by Wilson et al. (2014) [3]. The most irregular curved bridge with the highest length-to-radius ratio experiences the lowest average error between the exact and approximate IDA. However, a relatively large error in the 16th percentile of the three-span curved bridge with a curvature of 130 m indicates that the consistency of this approach is not simply related to the length-to-radius ratio and that the difference between the column heights plays an important role. As a result, the validity of this approach is different for each category in this study. In the four-span curved bridge category, the errors related to very weak or very strong ground motions (16th and 84th percentiles) increase from 5% to 17% with an increase in the radius of curvature to 1000 m, while the 50th percentile acts in the opposite way. The results are relatively different for two-span and three-span bridges; For these two categories with less irregularity than the other, the curved bridge with a radius of 420 m in two spans and the curved bridge with a radius of 1000 m in three spans experienced lower average errors in very strong motions (84th percentile) than the other curves. Furthermore, this approach led to perfectly consistent results for weaker earthquakes (84th and 50th percentiles) in the two-span curved bridge with the mentioned curvature, while stronger earthquakes (16th and 50th percentiles) were better predicted in the three-span curved bridge, indicating that the radius can affect the accuracy of the approach differently depending on the number of spans (length and irregularity). Therefore, both radius (R) and length (L) are used as important features in the following chapter.

5. References

1. Ali Naseri, A.R. M.Goltabar.R, Hossein Pahlavan and Gholamreza Ghodrati Amiri .2020. Effects of curvature radius on vulnerability of curved bridges subjected to near and far-field strong ground motions. Structural Monitoring and Maintenance 7(4):367-392.
2. Chiyu Jiao, Junrui Lu, Chuang Wang, Peiheng Long, Zhe Sun. 2021. Experimental and numerical investigations on the effects of radius of curvature and longitudinal slope on the responses of curved bridges subject to seismic pounding. Measurement and Control. Volume 54, Issue 3-4.
3. Wilson T, Mahmoud H, Chen S. 2014. Seismic performance of skewed and curved reinforced concrete bridges in mountainous states. *Eng Struct*: 70: 158–167.
4. Alireza Mirza Goltabar Roshan., Hossein Pahlavan., Gholamreza Ghodrati Amiri. Effect of curvature radius on probabilistic evaluation of seismic horizontally Curves RC Box girder bridges using Monte Carlo simulation under three-dimensional excitations under Near-Field Earthquakes. *Journal of Structural and Construction Engineering (JSCE)*, 2021. Volume 8, Issue 7. Pages 5-30.
5. Suyesha Agrawal and Praveen Kumar Gupta. 2024. Effect of radius of curvature on the seismic response of curved bridges. *IOP Conf. Ser.: Earth Environ. Sci*. 1326 012017.
6. Soleimani, S., Aziminejad, A., & Moghadam, A. S. (2017). Extending the concept of energy-based pushover analysis to assess seismic demands of asymmetric-plan buildings. Soil Dynamics and Earthquake Engineering, 93, 29-41.
7. Araújo, Miguel, Mário Marques, and Raimundo Delgado. (2014) "Multidirectional pushover analysis for seismic assessment of irregular-in-plan bridges." Engineering Structures 79: 375-389.
8. Pinto, A. V., Verzeletti, G., Magonette, G., Pegon, P., Negro, P., & Guedes, J. (1996). Pseudo-dynamic testing of large-scale R/C bridges in ELSA. In 11th world conference on earthquake engineering (pp. 23-28).
9. Akbari, R. (2012). Seismic fragility analysis of reinforced concrete continuous span bridges with irregular configuration. Structure and Infrastructure Engineering, 8(9), 873-889.
10. Tehrani, P., & Mitchell, D. (2021). Prediction of mean responses of RC bridges considering the incident angle of ground motions and displacement directions. Applied Sciences, 11(6), 2462.
11. Ramanathan, K., DesRoches, R., & Padgett, J. E. (2010). Analytical fragility curves for multispan continuous steel girder bridges in moderate seismic zones. Transportation Research Record, 2202(1), 173-182.
12. Ramanathan, K. N. (2012). Next generation seismic fragility curves for California bridges incorporating the evolution in seismic design philosophy. Georgia Institute of Technology.
13. Choi, E. (2002). Seismic analysis and retrofit of mid-America bridges. Georgia Institute of Technology.
14. Chang, G. A., & Mander, J. B. (1994). Seismic energy based fatigue damage analysis of bridge columns: Part I-Evaluation of seismic capacity (p. 222). Buffalo, NY: National Center for Earthquake Engineering Research.
15. Menegotto, M., Pinto, P. E. (1973). Method of Analysis for Cyclically Loaded Reinforced Concrete Plane Frames Including Changes in Geometry and Non-Elastic Behavior of Elements Under Combined Normal Force and Bending, Proceedings of the IABSE Symposium on Resistance and Ultimate Deformability of Structures Acted on by Well-Defined Repeated Loads, Lisbon, Portugal, pp: 15-22.
16. Filippou, F. C., Popov, E. P. Bertero, V. V. (1983). Effects of Bond Deterioration on Hysteretic Behavior of Reinforced Concrete Joints, Report No. EERC 83-19, Earthquake Engineering Research Center, University of California, Berkeley, CA.
17. Monteiro, Ricardo Nuno Carvalho. (2011) "Probabilistic seismic assessment of bridges." PhD diss., Universidade do Porto, Portugal.
18. Pahlavan, H., Zakeri, B., Amiri, G. G., & Shaianfar, M. (2015). Probabilistic vulnerability assessment of horizontally curved multiframe RC box-girder highway bridges. Journal of Performance of Constructed Facilities, 30(3), 04015038.